Microstructure and Hardness Evolution in Magnesium Processed by HPT

Cláudio L. P. Silva[1], Isabela C. Tristão[2], Shima Sabbaghianrad[3], Seyed A. Torbati-Sarraf[3], Roberto B. Figueiredo[4,*], Terence G. Langdon[5]

[1]Department of Metallurgical and Materials Engineering, Universidade Federal de Minas Gerais, Belo Horizonte 31270-901, Brazil

[2]Department of Mechanical Engineering, Universidade Federal de Minas Gerais, Belo Horizonte 31270-901, Brazil

[3]Departments of Aerospace and Mechanical Engineering & Materials Science, University of Southern California, Los Angeles, CA 90089-1453, U.S.A.

[4]Department of Materials Engineering and Civil Construction, Universidade Federal de Minas Gerais, Belo Horizonte 31270-901, Brazil

[5]Materials Research Group, Faculty of Engineering and the Environment, University of Southampton, Southampton SO17 1BJ, UK

[#]Corresponding author: figueiredo@demc.ufmg.br

Abstract

High pressure torsion provides an opportunity to process materials with low formability such as magnesium at room temperature. The present work shows the microstructure evolution in commercially pure magnesium processed using a pressure of 6.0GPa up to 10 turns of rotation. The microstructure evolution is evaluated using electron microscopy and the hardness is determined using dynamic hardness testing. The results show that the grain refinement mechanism in this material differs from materials with b.c.c. and f.c.c. structures. The mechanism of grain refinement observed at high temperatures also applies at room temperature. The hardness distribution is heterogeneous along the longitudinal section of the discs and is not affected by the amount of deformation imposed to the material.

Keywords: high-pressure torsion; magnesium; EBSD

1. Introduction

High-pressure torsion (HPT)[1, 2]is a metal processing technique in which a sample is subjected to torsion under elevated pressure. The pressure leads to high hydrostatic compressive stresses and severe plastic deformation is introduced by torsion increasing significantly the amount of crystalline defects in the material structure. Thus, a high dislocation density and an increased area of grain boundaries are observed in processed metallic materials leading to high strength and refined grain structures.

High pressure torsion has been widely used to process magnesium and its alloys at room temperature despite their low formability. Many papers have reported the formation of ultrafine grained structures in pure magnesium [3-6] and AZ31 [7-11], AZ61 [12], AZ80 [13], AZ91 [14-16], ZK60 [17-19], Mg-Zn-Y [20, 21], Mg-Gd-Y-Zr[22, 23], Mg-Zn-Ca [24-27] and Mg-Dy-Al-Zn-Zr[28]alloys. The processed alloys exhibit improved strength but also some papers report superplastic behaviour [16, 19, 22, 29, 30], improved hydrogen storage properties [3, 31-35] and improved corrosion resistance [24, 27, 36].

Formation of ultrafine grained structures and improved strength are also observed in other metallic materials processed by HPT. However, the evolution of the microstructure and the distribution of hardness in processed discs of magnesium and its alloys seem to differ from other f.c.c. and b.c.c. materials.It is expected that the amount of strain imposed to the disc during HPT processing is proportional to the distance from the center due to the torsional deformation. Thus, hardness variations along the sample radius are expected in the early stage of processing when the material has not reached hardness saturation. However, the amount of strain and the hardness are not expected to vary along the sample thickness and this has been confirmed by experiments in pure aluminium [37, 38] and iron[39]. Minor variations in distribution of strain along the sample thickness has been predicted by finite element modelling [40, 41] due

to friction and variations in hardness distribution have been reported in samples with low diameter to thickness ratio [39, 42]. However, experiments have shown significant heterogeneity in hardness distribution along the disc thickness in a magnesium alloy in samples with high diameter to thickness ratio[43, 44].

Moreover, it is known that the high amount of defects introduced by plastic deformation leads to the formation of low angle boundaries in the early stage of processing and the misorientation of these boundaries increase with continuing processing. Therefore, a large fraction of low angle boundaries are expected in the early stage of HPT processing and a gradual transition towards a larger fraction of high angle boundaries is expected at later stages. This has been confirmed by experiments in aluminium [45, 46] and in pure iron [47]. However, the mechanism of grain refinement in magnesium and its alloys differs from f.c.c. and b.c.c. materials. A mechanism in which new refined grains are formed along coarse grains boundaries has been proposed [48-50] based on experimental evidence of microstructure evolution for high temperature processing.

The understanding of the distribution of plastic deformation and evolution of structure during HPT processing is of key importance to future production of components of magnesium alloys with superior strength, superplastic properties, enhanced hydrogen storage kinetics or improved corrosion resistance. The present paper aims to clarify the distribution of hardness along the disc longitudinal plane using dynamic hardness measurements at different stages of HPT processing and to determine the evolution of grain boundary misorientation distribution.

2. Experimental material and procedures

The material used in the present work was commercial purity magnesium provided by RIMA (Bocaiúva / Brazil) as a cast slab. The material was machined into a billet with 10 mm

diameter and 100 mm length. Discs with 1 mm thickness were cut using a low speed diamond coated saw and were ground to ~0.85 mm thickness using abrasive papers.

The discs were processed by HPT using quasi-constrained anvils and a nominal pressure of 6.0GPa. The rotation rate was 1 rpm which is expected to lead to ~10 K temperature rise during processing (considering a flow stress of 200 MPa) [51, 52]. Discs were processed to 1/8, 1/2, 2 and 10 turns.

The distribution of hardness was determined on the longitudinal section of the discs. A low speed diamond coated saw was used to cut the discs and the samples were mounted using room temperature curing resin. The samples were ground and polished to a mirror-like finish. Figure 1 illustrates the section and the location of indentations. A Shimadzu DUH-211s dynamic hardness tester with a Berkovich indenter was used for testing. The maximum applied load was 200 mN, the loading rate was ~70 mN/s and the dwell time was set to 0 s in order to avoid room temperature creep which has been shown to take place in magnesium processed by HPT [6]. The values of hardness were plotted as colour coded maps as a function of the indentation position. Also, the average hardness for indentations at similar distance from the center were plotted as a function of the effective strain which was determined by the following equation [53, 54].

$$\varepsilon = \frac{2\pi N r}{t\sqrt{3}} \quad (1)$$

where N is the number of turns, r is the distance to the center and t is the sample thickness.

The microstructure was determined at mid-radius position (see Fig. 1) using EBSD. The samples were polished to a mirror-like finish using diamond paste and the final polishing step used colloidal silica in a Vibromet equipment. The equipment used for EBSD characterization was a JEOL JSM-7001F scanning electron microscope operating at 7 kV. The step size was 0.1 μm. The images were cleaned up using grain confidence index (CI) standardization, neighbor CI correlation and grain dilation procedures.

3. Results and discussion

3.1.Microstructure

Figure 2 shows representative images of the grain structure of samples processed by 1/8, 1/2 and 10 turns of HPT. Different colours are used to set apart low angle (red) and high angle (black) boundaries. Grains sizes with over one order of magnitude difference are clearly observed in the sample processed by 1/8 turn. The smaller grains are typically located between coarse grains suggesting they are formed along grain boundaries. The microstructure of the material processed by 1/2 turn exhibits grains with different sizes although the size difference between the small and coarse grains is reduced significantly. Also, the area fraction occupied by the coarse grains decreased significantly by comparison to the material processed by 1/8 turn.Finally, the microstructure of the material processed by 10 turns of HPT continues to exhibit a few coarse grains although it is apparent that the area fraction of the coarse grains is reduced. This is in agreement with transmission electron microscopy characterization of magnesium processed by HPT in which some coarser grains are observed in the microstructure even after multiple turns of processing [3, 6, 55]. Therefore, a mix of ultrafine grains and grains with a few microns of diameter seems to be a stable microstructure in pure magnesium processed by HPT.

In order to determine the area fraction occupied by coarse and fine grains at the different stages of processing, the cumulative distribution of grain sizes in samples processed by 1/8, 1/2 and 10 turns of HPT is shown in Fig. 3. It is observed that most of the microstructure is composed of grains larger than 1 micron in the sample processed by 1/8 turn. Processing to 1/2 turn increases significantly the area occupied by ultrafine grains and decreases the size of the largest grains. Further processing up to 10 turns does not change the distribution of the

very fine grains (<0.6 μm) but increased the fraction of grains in the range 0.6 μm ~ 1.0 μm and reduced the fraction of coarser grains. This is in agreement with the trend observed in magnesium processed by Equal-Channel Angular Pressing at high temperatures in which the new grains nucleate along grain boundaries and slowly consume the coarse grains [48-50].

Figure 4 shows the distribution of misorientation angles of the grain boundaries for the different samples. A large fraction (~0.41) of grain boundaries exhibit misorientations lower than 15º after only 1/8 turn but the frequency of low angle boundaries is decreased significantly after only 1/2 turn (~0.27). An additional decrease in frequency of low angle boundaries is observed after 10 turns which ultimately stabilizes in ~0.15. The frequency of low angle boundaries in magnesium is significantly lower than observed in other metallic materials [46, 47]. It is also worth noting a peak of frequency of boundaries between 85º ~ 90º which is associated with twinning [56] and a peak at ~30º which is associated with a basal texture [57].

3.2.Hardness

Figure 5 shows colour-coded distribution of hardness at the longitudinal sections of samples processed to 1/8, 1/2, 2 and 10 turns of HPT. It is observed that the hardness does not vary notably with the distance from the center and also does not vary with the number of turns although the amount of plastic strain imposed to the material by torsion increases linearly with increasing distance from the center and with the number of turns. The hardness maps show substantial variations in hardness without a clear trend. Areas with low hardness (~50 kgf mm^{-2}) and areas with high hardness (~65 kgf mm^{-2}) are observed throughout the longitudinal sections of the samples at the different stages of processing. This heterogeneous distribution of hardness differs from reports in purealuminum[38] and in pure iron [39] where

homogeneous distributions of hardness have been reported along the sample thickness and a clear trend is observed at different distances from the center.

Figure 6 shows the average hardness plotted as a function of the effective strain. It is observed that the hardness does not vary significantly with the amount of effective strain. Hardness values in the range 55 ~ 60kgf mm^2 are observed at strains in the range 0.3 ~ 200. This disagrees with a report in the literature of a peak hardness at low strains followed by slight softening and saturation [3]. The softening observed at intermediate values of strain in pure magnesium is usually attributed to the occurrence of recovery and recrystallization in this material [3]. However, the present results show that this may not be the case since softening was not observed in the present experiments. Recent reports have showed that pure magnesium exhibit an inverse Hall-Petch relation at very small grain sizes [58] and a change in deformation mechanism [6, 58] takes place at levels of strain in which the softening effect is usually observed. Grain boundary sliding starts to play a role in deformation leading to an apparent softening effect. Thus, the decrease in hardness is attributed to creep by grain boundary sliding during dwell time in conventional hardness testing. The indentations in the present work were controlled and the dwell time was removed in order to prevent creep and therefore the softening effect was not observed.

4. Summary and conclusions

1-High-pressure torsion was used to introduce severe plastic deformation in pure magnesium. EBSD characterization revealed the formation of small grains along grain boundaries of coarse grains. The fine grains gradually consume the coarse grains with increasing imposed strain.

2-The gradual increase in fraction of ultrafine grains and the fast evolution of the distribution of grain boundary misorientation towards high angles differs from other metallic materials and agrees with a model of grain refinement for magnesium processed at high temperatures.

3-The distribution of hardness is heterogeneous along the longitudinal plane of the processed disc which also differs from other metallic materials.

4-The average hardness does not vary with the amount of imposed effective strain during HPT. The softening effect reported in the literature is attributed to the onset of grain boundary sliding and creep during dwell time in conventional hardness testing.

5. Acknowledgements

The authors acknowledge support from CNPq, FAPEMIG and CAPES. One of the authors acknowledges support from the European Research Council under ERC Grant Agreement No. 267464-SPDMETALS (TGL).

6. References

1. Zhilyaev AP, Langdon TG. Using high-pressure torsion for metal processing: Fundamentals and applications. Progress in Materials Science. 2008;53(6):893-979.
2. Figueiredo RB, Cetlin PR, Langdon TG. Using finite element modeling to examine the flow processes in quasi-constrained high-pressure torsion. Materials Science and Engineering: A. 2011;528(28):8198-204.
3. Edalati K, Yamamoto A, Horita Z, Ishihara T. High-pressure torsion of pure magnesium: Evolution of mechanical properties, microstructures and hydrogen storage capacity with equivalent strain. Scripta Materialia. 2011;64(9):880-3.
4. Figueiredo RB, Aguilar MTP, Cetlin PR, Langdon TG. Processing magnesium alloys by severe plastic deformation. In: Beausir B, Bouaziz O, Bouzy E, Grosdidier T, Toth LS, editors. 6th International Conference on Nanomaterials by Severe Plastic Deformation. IOP Conference Series-Materials Science and Engineering. 632014.
5. Figueiredo RB, Poggiali FSJ, Silva CLP, Cetlin PR, Langdon TG. The influence of grain size and strain rate on the mechanical behavior of pure magnesium. Journal of Materials Science. 2016;51(6):3013-24.
6. Figueiredo RB, Sabbaghianrad S, Giwa A, Greer JR, Langdon TG. Evidence for exceptional low temperature ductility in polycrystalline magnesium processed by severe plastic deformation. Acta Materialia. 2017;122:322-31.

7. Huang Y, Figueiredo RB, Baudin T, Brisset F, Langdon TG. Evolution of Strength and Homogeneity in a Magnesium AZ31 Alloy Processed by High-Pressure Torsion at Different Temperatures. Advanced Engineering Materials. 2012;14(11):1018-26.
8. Huang Y, Figueiredo RB, Baudin T, Helbert AL, Brisset F, Langdon TG. Microstructure and Texture Evolution in a Magnesium Alloy During Processing by High-Pressure Torsion. Materials Research-Ibero-American Journal of Materials. 2013;16(3):577-85.
9. Serre P, Figueiredo RB, Gao N, Langdon TG. Influence of strain rate on the characteristics of a magnesium alloy processed by high-pressure torsion. Materials Science and Engineering: A. 2011;528(10-11):3601-8.
10. Stráská J, Janeček M, Gubicza J, Krajňák T, Yoon EY, Kim HS. Evolution of microstructure and hardness in AZ31 alloy processed by high pressure torsion. Materials Science and Engineering: A. 2015;625:98-106.
11. Xu J, Wang X, Shirooyeh M, Xing G, Shan D, Guo B, et al. Microhardness, microstructure and tensile behavior of an AZ31 magnesium alloy processed by high-pressure torsion. Journal of Materials Science. 2015;50(22):7424-36.
12. Harai Y, Kai M, Kaneko K, Horita Z, Langdon TG. Microstructural and Mechanical Characteristics of AZ61 Magnesium Alloy Processed by High-Pressure Torsion. MATERIALS TRANSACTIONS. 2008;49(1):76-83.
13. Alsubaie SA, Bazarnik P, Lewandowska M, Huang Y, Langdon TG. Evolution of microstructure and hardness in an AZ80 magnesium alloy processed by high-pressure torsion. Journal of Materials Research and Technology. 2016;5(2):152-8.
14. Al-Zubaydi A, Figueiredo RB, Huang Y, Langdon TG. Structural and hardness inhomogeneities in Mg-Al-Zn alloys processed by high-pressure torsion. Journal of Materials Science. 2013;48(13):4661-70.
15. Al-Zubaydi ASJ, Zhilyaev AP, Wang SC, Kucita P, Reed PAS. Evolution of microstructure in AZ91 alloy processed by high-pressure torsion. Journal of Materials Science. 2016;51(7):3380-9.
16. Al-Zubaydi ASJ, Zhilyaev AP, Wang SC, Reed PAS. Superplastic behaviour of AZ91 magnesium alloy processed by high-pressure torsion. Materials Science and Engineering: A. 2015;637:1-11.
17. Galiyev A, Kaibyshev R. Microstructural Evolution in ZK60 Magnesium Alloy during Severe Plastic Deformation. MATERIALS TRANSACTIONS. 2001;42(7):1190-9.
18. Lee H-J, Lee SK, Jung KH, Lee GA, Ahn B, Kawasaki M, et al. Evolution in hardness and texture of a ZK60A magnesium alloy processed by high-pressure torsion. Materials Science and Engineering: A. 2015;630:90-8.
19. Torbati-Sarraf SA, Langdon TG. Properties of a ZK60 magnesium alloy processed by high-pressure torsion. Journal of Alloys and Compounds. 2014;613:357-63.
20. Basha DA, Sahara R, Somekawa H, Rosalie JM, Singh A, Tsuchiya K. Interfacial segregation induced by severe plastic deformation in a Mg–Zn–Y alloy. Scripta Materialia. 2016;124:169-73.
21. Jenei P, Gubicza J, Yoon EY, Kim HS. X-ray diffraction study on the microstructure of a Mg–Zn–Y alloy consolidated by high-pressure torsion. Journal of Alloys and Compounds. 2012;539:32-5.
22. Alizadeh R, Mahmudi R, Ngan AHW, Huang Y, Langdon TG. Superplasticity of a nano-grained Mg–Gd–Y–Zr alloy processed by high-pressure torsion. Materials Science and Engineering: A. 2016;651:786-94.

23. Dobatkin SV, Rokhlin LL, Lukyanova EA, Murashkin MY, Dobatkina TV, Tabachkova NY. Structure and mechanical properties of the Mg-Y-Gd-Zr alloy after high pressure torsion. Materials Science and Engineering: A. 2016;667:217-23.
24. Gao JH, Guan SK, Ren ZW, Sun YF, Zhu SJ, Wang B. Homogeneous corrosion of high pressure torsion treated Mg–Zn–Ca alloy in simulated body fluid. Materials Letters. 2011;65(4):691-3.
25. Kulyasova OB, Islamgaliev RK, Zhao Y, Valiev RZ. Enhancement of the Mechanical Properties of an Mg–Zn–Ca Alloy Using High-Pressure Torsion. Advanced Engineering Materials. 2015;17(12):1738-41.
26. Kulyasova O, Islamgaliev R, Zhao Y, Valiev R. Microstructure and mechanical properties of ultrafinegrained Mg-Zn-Ca alloy. IOP Conference Series: Materials Science and Engineering. 2014;63(1):012142.
27. Zhang CZ, Zhu SJ, Wang LG, Guo RM, Yue GC, Guan SK. Microstructures and degradation mechanism in simulated body fluid of biomedical Mg–Zn–Ca alloy processed by high pressure torsion. Materials & Design. 2016;96:54-62.
28. Kocich R, Kunčická L, Král P, Lowe TC. Texture, deformation twinning and hardening in a newly developed Mg–Dy–Al–Zn–Zr alloy processed with high pressure torsion. Materials & Design. 2016;90:1092-9.
29. Kai M, Horita Z, Langdon TG. Developing grain refinement and superplasticity in a magnesium alloy processed by high-pressure torsion. Materials Science and Engineering: A. 2008;488(1–2):117-24.
30. Matsunoshita H, Edalati K, Furui M, Horita Z. Ultrafine-grained magnesium–lithium alloy processed by high-pressure torsion: Low-temperature superplasticity and potential for hydroforming. Materials Science and Engineering: A. 2015;640:443-8.
31. Gajdics M, Calizzi M, Pasquini L, Schafler E, Révész Á. Characterization of a nanocrystalline Mg–Ni alloy processed by high-pressure torsion during hydrogenation and dehydrogenation. International Journal of Hydrogen Energy. 2016;41(23):9803-9.
32. Grill A, Horky J, Panigrahi A, Krexner G, Zehetbauer M. Long-term hydrogen storage in Mg and ZK60 after Severe Plastic Deformation. International Journal of Hydrogen Energy. 2015;40(47):17144-52.
33. Hongo T, Edalati K, Arita M, Matsuda J, Akiba E, Horita Z. Significance of grain boundaries and stacking faults on hydrogen storage properties of Mg2Ni intermetallics processed by high-pressure torsion. Acta Materialia. 2015;92:46-54.
34. Leiva DR, Jorge AM, Ishikawa TT, Huot J, Fruchart D, Miraglia S, et al. Nanoscale Grain Refinement and H-Sorption Properties of MgH2 Processed by High-Pressure Torsion and Other Mechanical Routes. Advanced Engineering Materials. 2010;12(8):786-92.
35. Soyama J, Floriano R, Leiva DR, Guo Y, Jorge Junior AM, Pereira da Silva E, et al. Severely deformed ZK60 + 2.5% Mm alloy for hydrogen storage produced by two different processing routes. International Journal of Hydrogen Energy. 2016;41(26):11284-92.
36. Silva CLP, Oliveira AC, Costa CGF, Figueiredo RB, de Fátima Leite M, Pereira MM, et al. Effect of severe plastic deformation on the biocompatibility and corrosion rate of pure magnesium. Journal of Materials Science. 2017:in press.
37. Kawasaki M, Figueiredo RB, Langdon TG. An investigation of hardness homogeneity throughout disks processed by high-pressure torsion. Acta Materialia. 2011;59(1):308-16.
38. Kawasaki M, Figueiredo RB, Langdon TG. Twenty-five years of severe plastic deformation: recent developments in evaluating the degree of homogeneity through the

thickness of disks processed by high-pressure torsion. Journal of Materials Science. 2012;47(22):7719-25.
39. Hohenwarter A, Bachmaier A, Gludovatz B, Scheriau S, Pippan R. Technical parameters affecting grain refinement by high pressure torsion. Int J Mater Res. 2009;100(12):1653-61.
40. Figueiredo RB, Aguilar MTP, Cetlin PR, Langdon TG. Analysis of plastic flow during high-pressure torsion. Journal of Materials Science. 2012;47(22):7807-14.
41. Figueiredo RB, de Faria GCV, Cetlin PR, Langdon TG. Three-dimensional analysis of plastic flow during high-pressure torsion. Journal of Materials Science. 2013;48(13):4524-32.
42. Sakai G, Nakamura K, Horita Z, Langdon TG. Developing high-pressure torsion for use with bulk samples. Materials Science and Engineering: A. 2005;406(1–2):268-73.
43. Figueiredo RB, Langdon TG. Heterogeneous Flow During High-Pressure Torsion. Materials Research-Ibero-American Journal of Materials. 2013;16(3):571-6.
44. Figueiredo RB, Langdon TG. Development of structural heterogeneities in a magnesium alloy processed by high-pressure torsion. Materials Science and Engineering: A. 2011;528(13-14):4500-6.
45. Xu C, Horita Z, Langdon TG. Microstructural Evolution in Pure Aluminum in the Early Stages of Processing by High-Pressure Torsion. MATERIALS TRANSACTIONS. 2010;51(1):2-7.
46. Ito Y, Horita Z. Microstructural evolution in pure aluminum processed by high-pressure torsion. Materials Science and Engineering: A. 2009;503(1–2):32-6.
47. Ivanisenko Y, Valiev RZ, Fecht HJ. Grain boundary statistics in nano-structured iron produced by high pressure torsion. Materials Science and Engineering: A. 2005;390(1–2):159-65.
48. Figueiredo RB, Langdon TG. Grain refinement and mechanical behavior of a magnesium alloy processed by ECAP. Journal of Materials Science. 2010;45(17):4827-36.
49. Figueiredo RB, Langdon TG. The nature of grain refinement in equal-channel angular pressing: a comparison of representative fcc and hcp metals. Int J Mater Res. 2009;100(12):1638-46.
50. Figueiredo RB, Langdon TG. Principles of grain refinement in magnesium alloys processed by equal-channel angular pressing. Journal of Materials Science. 2009;44(17):4758-62.
51. Figueiredo RB, Pereira PHR, Aguilar MTP, Cetlin PR, Langdon TG. Using finite element modeling to examine the temperature distribution in quasi-constrained high-pressure torsion. Acta Materialia. 2012;60(6-7):3190-8.
52. Pereira PHR, Figueiredo RB, Huang Y, Cetlin PR, Langdon TG. Modeling the temperature rise in high-pressure torsion. Materials Science and Engineering: A. 2014;593:185-8.
53. Jonas JJ, Ghosh C, Toth LS. The equivalent strain in high pressure torsion. Materials Science and Engineering: A. 2014;607:530-5.
54. Valiev RZ, Ivanisenko YV, Rauch EF, Baudelet B. Structure and deformaton behaviour of Armco iron subjected to severe plastic deformation. Acta Materialia. 1996;44(12):4705-12.
55. Bonarski BJ, Schafler E, Mingler B, Skrotzki W, Mikulowski B, Zehetbauer MJ. Texture evolution of Mg during high-pressure torsion. Journal of Materials Science. 2008;43(23):7513.

56. Partridge PG. The crystallography and deformation modes of hexagonal close-packed metals. Metallurgical Reviews. 1967;12(1):169-94.
57. del Valle JA, Pérez-Prado MT, Ruano OA. Distribución de ángulos de desorientación en la aleación de Mg laminada AZ31. 2002. 2002;38(5):5.
58. Somekawa H, Mukai T. Hall-Petch Breakdown in Fine-Grained Pure Magnesium at Low Strain Rates. Metallurgical and Materials Transactions A. 2015;46A(2):894-902.

Figure captions

Figure 1 – Illustration of the section used for hardness testing, location of indentations and the location for EBSD characterization of the microstructure.

Figure 2 – Distribution of low angle (red) and high angle (black) boundaries in samples processed by 1/8, 1/2 and 10 turns of HPT.

Figure 3 – Cumulative fraction of grain sizes at different stages of processing.

Figure 4 – Frequency distribution of misorientation angles of grain boundaries.

Figure 5 – Distribution of hardness at the longitudinal section of discs processed by HPT to 1/8, 1/2, 2 and 10 turns.

Figure 6 – Distribution of hardness as a function of the imposed effective strain in HPT.

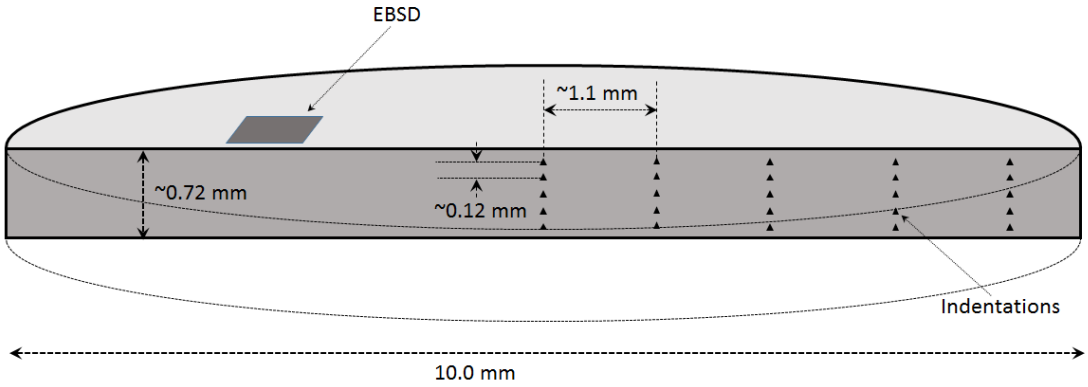

Figure 1 – Illustration of the section used for hardness testing, location of indentations and the location for EBSD characterization of the microstructure.

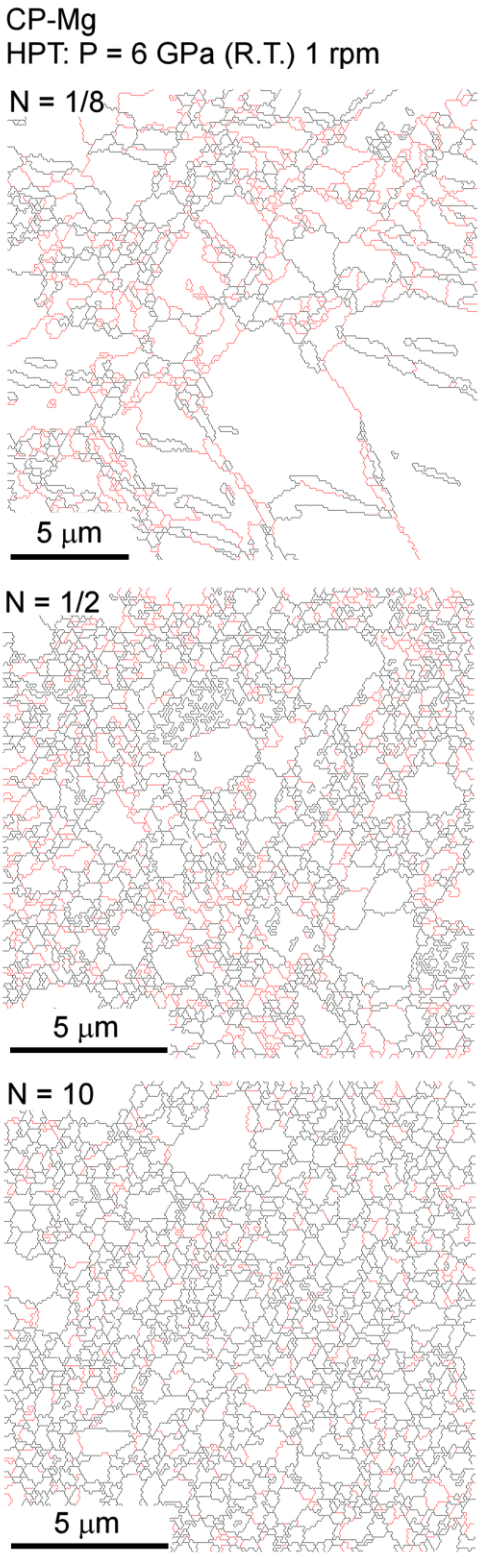

Figure 2 – Distribution of low angle (red) and high angle (black) boundaries in samples processed by 1/8, 1/2 and 10 turns of HPT.

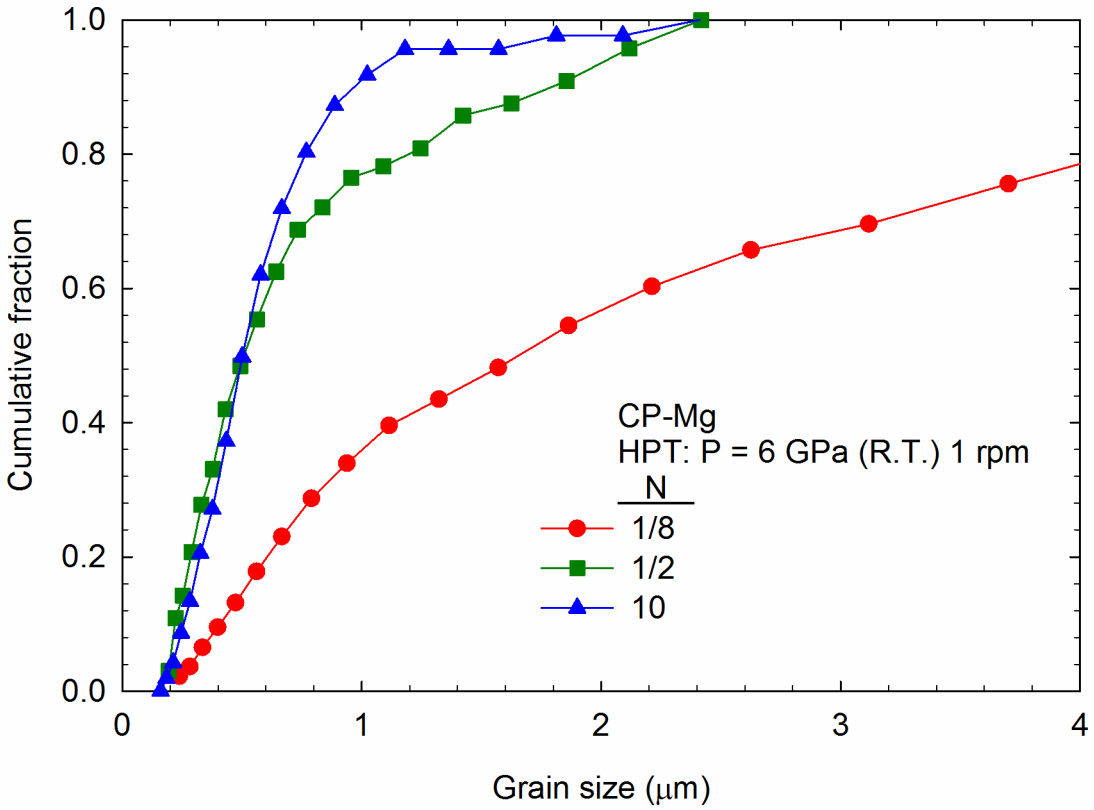

Figure 3 – Cumulative fraction of grain sizes at different stages of processing.

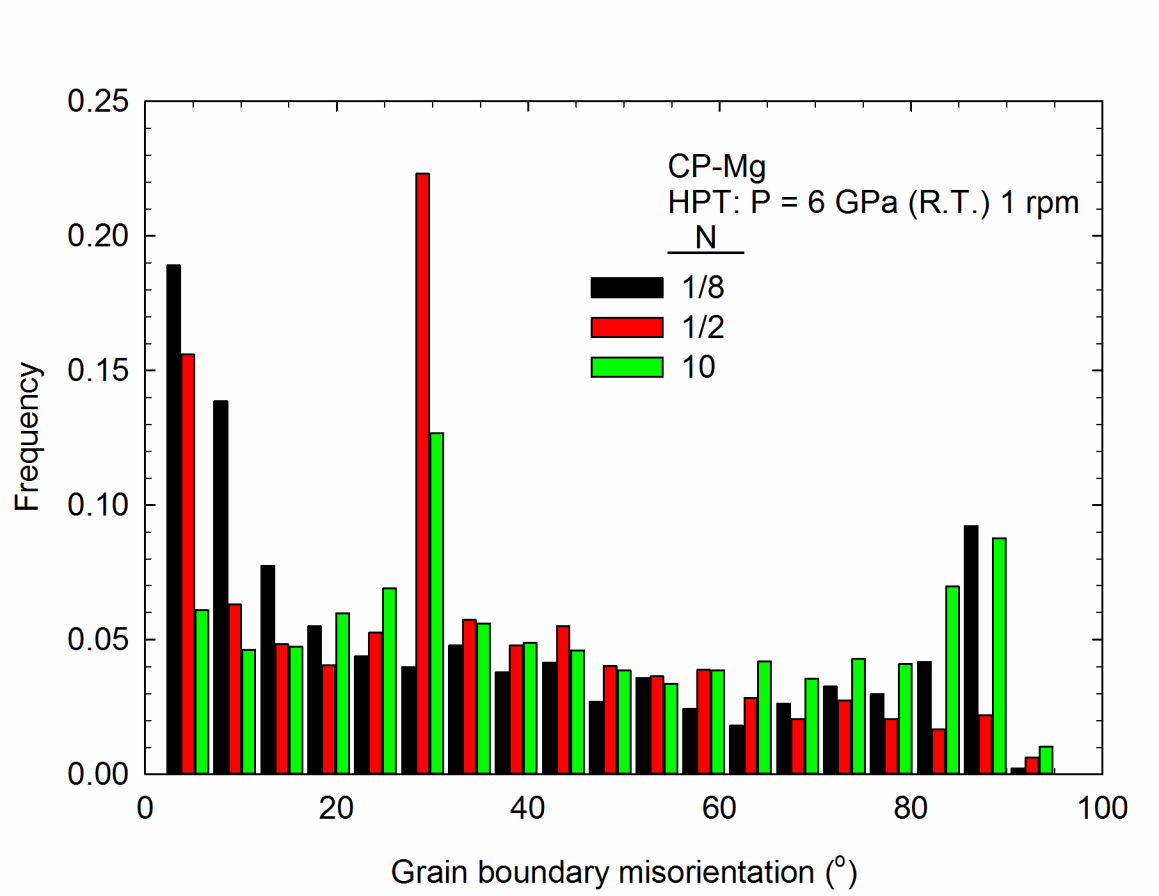

Figure 4 – Frequency distribution of misorientation angles of grain boundaries.

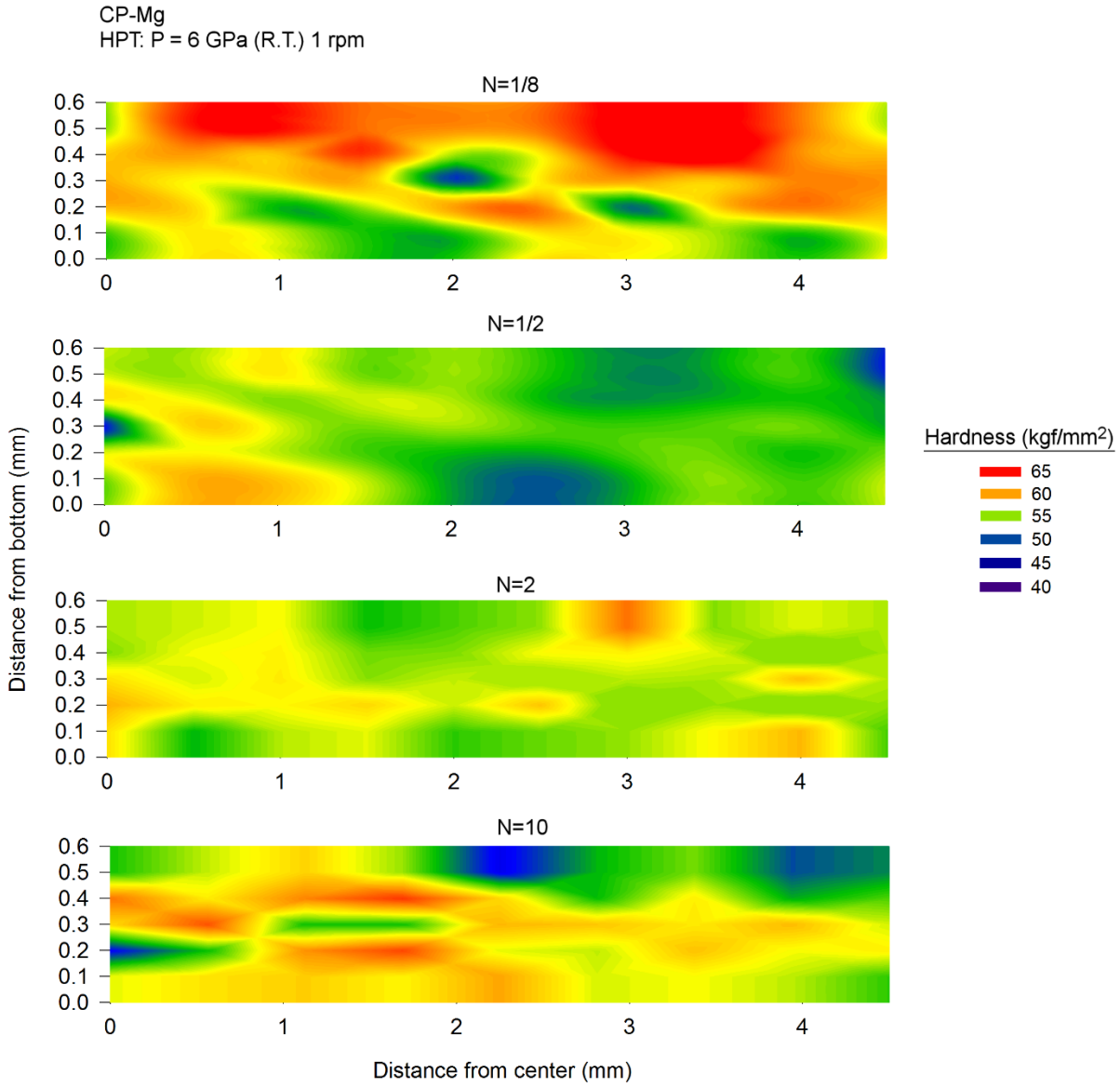

Figure 5 – Distribution of hardness at the longitudinal section of discs processed by HPT to 1/8, 1/2, 2 and 10 turns.

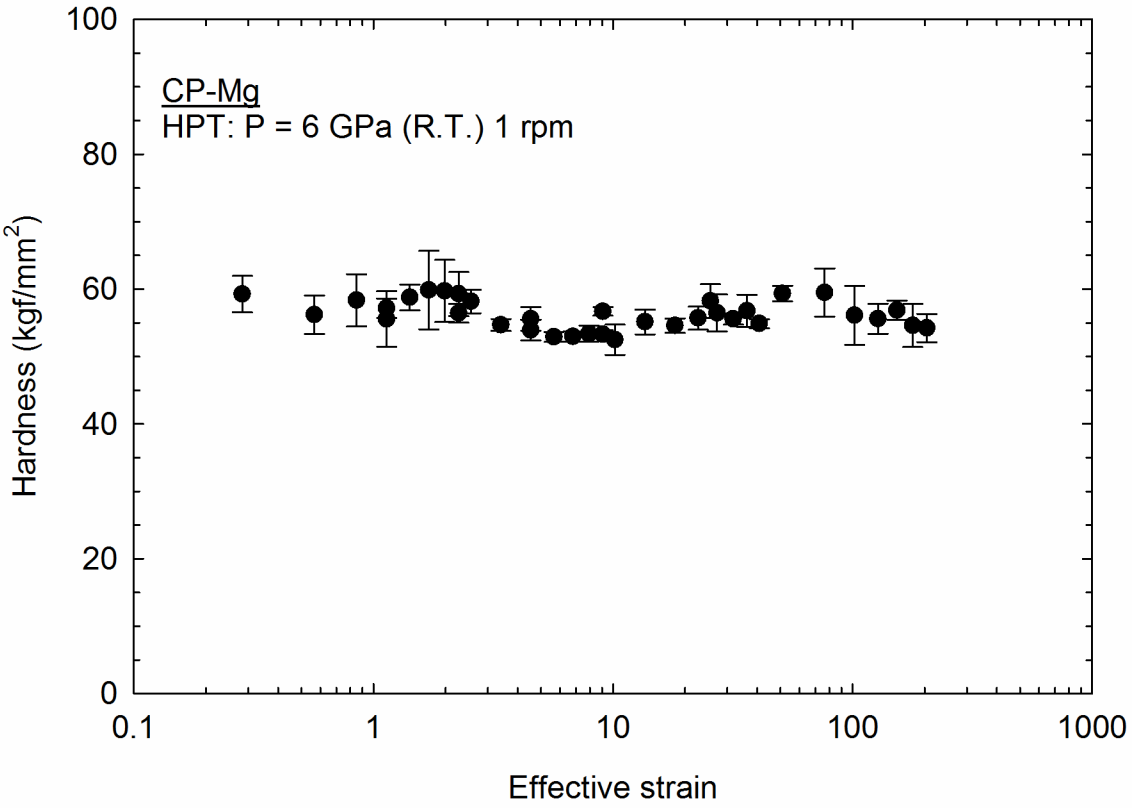

Figure 6 – Distribution of hardness as a function of the imposed effective strain in HPT.